NUMERICAL AND ANALYTICAL COMPARISONS OF SLANTED LORENTZ FORCES ON THERMAL RADIATION FLOW OF A MICROPOLAR FLUID

by

Elangovan RAMYA[a], Murugan MUTHTAMILSELVAN[a], Deog-Hee DOH[b], and Gyeong-Rae CHO[b]*

[a] Department of Mathematics, Bharathiar University, Coimbatore, Tamilnadu, India
[b] Division of Mechanical Engineering, College of Engineering,
Korea Maritime and Ocean University, Busan, South Korea

The transient flow of a viscous incompressible electrically conducting micro--stretch fluid over an infinite vertical porous plate in the presence of slanted hydromagnetic flow with an aligned angle of 0° to 90° and thermal radiation effects has been analyzed. The governing equations are solved analytically by using the technique of the state-space approach and the inversion of the Laplace transforms is carried out using a numerical approach for varies physical parameters on the velocity, microrotation, micro-stretch and temperature profiles are shown graphically. In order to verify the accuracy of the present results, we have compared these results with the numerical solution by using the Crank-Nicolson implicit finite difference method. It is found that the thickness of thermal boundary--layer increases with an increase in the value of thermal radiation whereas antithesis trend is seen with increasing the Prandtl number.
Key words: *slanted MHD, natural convection, microstretch fluid,*
porous medium, state-space approach, Crank-Nicolson

Introduction

The philosophy of micro-stretch fluids contains micropolar and moreover stretch was initiated by Eringen [1] as a subclass of the more common description of fluids known as simple micro-fluids, further known as Eringen fluids [2]. The micro-stretch fluid have a local substructure, whose material particles or micro elements have seven degrees of freedom, three of translation, three of rotation, and one of stretch or axial motion, consisting of expansions and contractions, at the same time the micropolar fluids whose particles are rigid, possess only six degrees of freedom, three of translation and three of rotation. In addition, micro-stretch fluids similar to micropolar fluids can support couple stresses and possess micro-inertia. We observed that the exclusive theory declared ahead can besides be applied, in the limiting action, to cover the classical Navier-Stokes fluid as well. There are plenty of articles on micro--stretch fluid model available [3-5], but most of them describe the natural convection flows of the micro-stretch fluid. Ezzat and El-Sapa [6] examined the free convection boundary-layer flow of a perfect conducting MHD micropolar fluid with stretch for the 1-D problem. For some MHD relevant work of interest we refer to [7-9]. By applying state space method and an

---

inversion Laplace transform, Helmy *et al.* [10] examined the 1-D hydromagnetic free convection flow of a micropolar fluid through a porous medium, past an illimitable vertical plate with uniform heating.

Then again, radiation impacts can be very huge in space technology applications and at higher operating temperatures. Heat transfer by concurrent radiation and convection has applications in various innovation issues including burning, furnace design, the configuration of high temperature gas cooled in nuclear reactors, nuclear reactor safety, fluidized bed heat exchanger, fire spreads, solar fans, solar collectors, natural convection in cavities, turbid water bodies, photo chemical reactors and numerous others. Pal and Chatterjee [11] has examined the heat transfer of a micropolar fluid saturated porous medium past an impermeable stretching sheet with magnetic field and thermal radiation effects utilizing the Darcy-Brinkman-Forchheirmer model. Ibrahim *et al.* [12] considered an impact of chemical reaction and radiation ingestion on the unsteady MHD free convection flow past a semi-infinite vertical permeable moving plate with heat source and suction. Radiation effect on a micropolar fluid through a permeable medium with or without magnetic field has been considered by various researchers [13-18].

The objective of the present work is to examine the effect of thermal radiation and slanted magnetic field on the boundary-layer flow of a micropolar fluid with stretch past a vertical porous plate. We analyze the problem through the method of state-space formulation, which is more general than the classical Laplace transform and Fourier transform techniques. The state-space hypothesis is pertinent to all frameworks that can be scrutinized by integral transforms in time and is effectively utilized to examine, in specifically, problems in modern control theory. The state-space formulation in micro-polar fluid problem was introduced by Ezzat *et al.* [19]. In this aspect, the governing equations are create in matrix form utilizing a state vector that comprises the Laplace transforms in time of the temperature, velocity, micro-rotation, micro-stretch, temperature and their gradients. Their integration subjected to zero initial condition is done by the method of matrix exponential technique. Influence functions in the Laplace transform domain are clearly formed. The resulting formulation is connected to a thermal shock problem with in the presence of a slanted magnetic field and thermal radiation. The inversion of the Laplace transform is carried out to utilize a numerical technique [20]. In addition, the Crank-Nicolson technique for stability and convergence finite difference scheme was also performed in the present work. A fine solution is obtained between both systematic and numerical techniques.
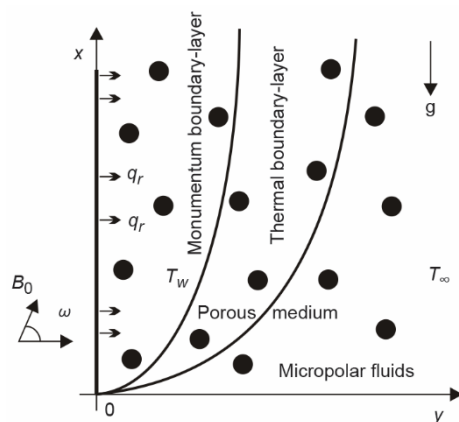

Figure 1. Physical configuration and co-ordinate system

Mathematical formulation

Consider a transient, laminar, 1-D natural convection flow of an incompressible, Micro-stretch fluid through an infinite vertical porous plate. Aligned magnetic field of potency B_0 is attached along with y direction, with an intense angle ω. At $\omega = 90°$ this magnetic field performance similar to transverse magnetic field (since sin $90° = 1$). It is further assumed that the induced magnetic field is negligible in comparison to the applied magnetic field. Let *x*-axis be along the surface, *y*-axis being normal to it. The physical model is delineated in fig. 1. The velocity components of the liquid are $q = (u, 0, 0)$ and the microrotation

Ramya, E., *et al.*: Numerical and Analytical Comparisons of Slanted …
THERMAL SCIENCE: Year 2019, Vol. 23, No. 2B, pp. 913-928

915

vector acting along z-axis $\Omega = (0, 0, \Omega)$. The scalar micro-inertia and all fluid properties are assumed constant except that the influence of the density variation with temperature is considered only in the body force term. The effect of the density variations in other terms of equations, are considered negligible. This is the well-known *Boussinesq approximation*. The system of equations which govern the transient natural convection stream of a micro-stretch conducting liquid, through a porous medium, past an impulsively infinite plate, when the velocity, microrotation, micro-stretch and temperature are functions of y and time t, are:

$$\frac{\partial v}{\partial y} = 0 \tag{1}$$

$$\frac{1}{\alpha}\frac{\partial v}{\partial y} + v\frac{\partial u}{\partial y} = v\frac{\partial^2 u}{\partial y^2} + v_1\frac{\partial N}{\partial y} + g\beta_T (T - T_\infty) - \frac{\sigma B_0^2 u}{\rho}\sin^2\omega - \frac{vu}{K_0} \tag{2}$$

$$j\left(\frac{1}{\alpha}\frac{\partial N}{\partial t} + v\frac{\partial N}{\partial y}\right) = \frac{\gamma}{\rho}\frac{\partial^2 N}{\partial y^2} - v_1\left(2N + \frac{\partial u}{\partial y}\right) \tag{3}$$

$$\frac{j}{2}\left(\frac{1}{\alpha}\frac{\partial \Omega}{\partial t} + v\frac{\partial \Omega}{\partial y}\right) = \frac{a_0}{\rho}\frac{\partial^2 \Omega}{\partial y^2} + \frac{\tau_1}{\rho}\frac{\partial^2 T}{\partial y^2} - \frac{(\eta_0 - \lambda_0)}{\rho}\Omega \tag{4}$$

$$\frac{1}{\alpha}\frac{\partial T}{\partial t} + v\frac{\partial T}{\partial y} = \frac{1}{\rho C_p}\left(\lambda\frac{\partial^2 T}{\partial y^2} - \frac{\partial q_r}{\partial y}\right) \tag{5}$$

where, u and v are the velocity components in the x- and y-directions, respectively, β_T – the coefficients of thermal expansion, N – the microrotation, Ω – the micro-stretch, T – the liquid temperature, α – the porosity, λ – the thermal conductivity, C_p – the specific heat at constant pressure, and μ, χ, γ, and j – the characteristic constants of the micropolar liquid, where $v_1 = \chi/\rho$, $v = (\mu + \chi)/\rho$ is the evident kinematic viscosity. The a_0, λ_0, and η_0 are micro-stretch viscosity moduli, τ_1 – micro-rotation heat conduction moduli.

The Rosseland diffusion approximation for radiation [7] heat flux is given by:

$$q_r = \frac{-4\sigma}{3k}\frac{\partial T^4}{\partial y}$$

where σ is the Stefan-Boltzmann constant, and k – the mean absorption coefficient. Further, we assume that the temperature difference within flow is such that T^4 may be expanded in a Taylor series. Hence expanding T^4 about T_∞ and dismissing higher order terms we get $T^4 = 4T_\infty^3 T - 3T_\infty^4$.

Hence:

$$\frac{\partial q_r}{\partial y} = \frac{-16T_\infty^3\sigma}{3k}\frac{\partial^2 T}{\partial y^2} \tag{6}$$

By utilizing eqs. (5) and (6), we get:

916

Ramya, E., *et al.*: Numerical and Analytical Comparisons of Slanted …
THERMAL SCIENCE: Year 2019, Vol. 23, No. 2B, pp. 913-928

$$\frac{1}{\alpha}\frac{\partial T}{\partial t} + v\frac{\partial T}{\partial y} = \frac{1}{\rho C_p}\lambda\frac{\partial^2 T}{\partial y^2} + \frac{1}{\rho C_p}\frac{16 T_\infty^3 \sigma}{3k\lambda}\frac{\partial^2 T}{\partial y^2} \tag{7}$$

Proceeding with the analysis, we state the non-dimensional quantities:

$$\left.\begin{array}{l} u' = \dfrac{u}{U}, \qquad y' = \dfrac{U}{v}y, \qquad N' = \dfrac{v}{U^2}N, \qquad \theta = \dfrac{T - T_\infty}{T_w - T_\infty}, \quad M_1 = \dfrac{\sigma B_0^2 v}{\rho U^2} \\[3mm] \Omega' = \dfrac{v}{U^2}\Omega, \qquad R_0 = \dfrac{jv}{\gamma/\rho}, \qquad R = \dfrac{v_1 v^2}{U^2(v/\rho)}, \quad t' = \dfrac{\alpha U^2}{v}t, \qquad G = \dfrac{v_1}{v}, \\[3mm] K = \dfrac{U^2}{v^2}K_0, \qquad \mathrm{Pr} = \dfrac{vC_p\rho}{\lambda}, \quad \mathrm{Gr} = \dfrac{g\beta_T v(T_w - T_\infty)}{U^3} \end{array}\right\} \tag{8}$$

where K_0 and M_1 are the permeability and magnetic parameter, respectively, G and F – the non-dimensional and radiation parameter, respectively, Pr – the Prandtl number, Gr – the Grashof number for heat transfer, subscripts w and ∞ refer to the quantities on the wall and far from the wall, respectively. If view of $v = 0$ invoking the previously non-dimensional quantities, eqs. (2)-(4) and (7) are reduced to the non-dimensional equations, dropping the asterisks for convenience:

$$\frac{\partial u}{\partial t} = \frac{\partial^2 u}{\partial y^2} + G\frac{\partial N}{\partial y} + \mathrm{Gr}\,\theta - Mu \tag{9}$$

$$R_0\frac{\partial N}{\partial t} = \frac{\partial^2 N}{\partial y^2} - R\left(2N + \frac{\partial u}{\partial y}\right) \tag{10}$$

$$\frac{R_1}{2}\frac{\partial \Omega}{\partial t} = R_2\frac{\partial^2 \Omega}{\partial y^2} + R_3\frac{\partial^2 \theta}{\partial y^2} - R_4\Omega \tag{11}$$

$$\frac{\partial \theta}{\partial t} = \frac{1}{\mathrm{Pr}}\frac{\partial^2 \theta}{\partial y^2} + \frac{4}{3}\frac{1}{\mathrm{Pr}}\frac{\partial^2 \theta}{\partial y^2}F \tag{12}$$

where

$$F = \frac{4T_\infty^3 \sigma}{k\lambda}, \quad M = M_1\sin^2\omega + \frac{1}{K}, \quad R_1 = \frac{U^2 j\rho v}{\gamma}, \quad R_2 = \frac{a_0 v U^2}{\gamma},$$

$$R_3 = \frac{\tau_1 v}{\gamma}(T_w - T_\infty), \quad R_4 = \frac{v^2}{\gamma}(\eta_0 - \lambda_0) \tag{13}$$

These equations will be supplemented with appropriate boundary condition relevant to the particular application under consideration, as will be seen. Taking the Laplace-transform, defined by the relation:

$$\bar{f}(s) = \int\limits_0^\infty e^{-st} f(t)\mathrm{d}t$$

Acting on both sides of eqs. (9)-(12) with considered the zero initial conditions, we obtain:

$$\frac{\mathrm{d}^2\bar{u}}{\mathrm{d}y^2} = (s+M)\bar{u} - \mathrm{Gr}\,\bar{\theta} - G\frac{\mathrm{d}\bar{N}}{\mathrm{d}y} \tag{14}$$

$$\frac{\mathrm{d}^2\bar{N}}{\mathrm{d}y^2} = (R_0 s + 2R)\bar{N} + R\frac{\mathrm{d}\bar{u}}{\mathrm{d}y} \tag{15}$$

$$R_2\frac{\mathrm{d}^2\bar{\Omega}}{\mathrm{d}y^2} = \frac{R_1}{2}s\bar{\Omega} - R_3\frac{\mathrm{d}^2\bar{\theta}}{\mathrm{d}y^2} + R_4\bar{\Omega} \tag{16}$$

$$\frac{\mathrm{d}^2\bar{\theta}}{\mathrm{d}y^2} = \mathrm{Pr}\,s\bar{\theta}\left(1+\frac{4F}{3}\right)^{-1} \tag{17}$$

State space formulation

We choose as state variable in the physical domain the quantities:

$$\bar{\theta}(y,t),\quad \bar{u}(y,t),\quad \bar{N}(y,t),\quad \bar{\Omega}(y,t),\quad \bar{\theta}'(y,t),\quad \bar{u}'(y,t),\quad \bar{N}'(y,t),\quad \text{and}\quad \bar{\Omega}'(y,t)$$

the state variable in the transformed domain are taken:

$$\bar{\theta}(y,s),\quad \bar{u}(y,s),\quad \bar{N}(y,s),\quad \bar{\Omega}(y,s),\quad \bar{\theta}'(y,s),\quad \bar{u}'(y,s),\quad \bar{N}'(y,s),\quad \text{and}\quad \bar{\Omega}'(y,s)$$

where the over bar means the Laplace transform, and the prime indicates differentiation with respect to *y*. Equations (14)-(17) can be written as:

$$\frac{\mathrm{d}}{\mathrm{d}y}\begin{bmatrix}\bar{\theta}\\\bar{u}\\\bar{N}\\\bar{\Omega}\\\bar{\theta}'\\\bar{u}'\\\bar{N}'\\\bar{\Omega}'\end{bmatrix} = \begin{bmatrix}0 & 0 & 0 & 0 & 1 & 0 & 0 & 0\\0 & 0 & 0 & 0 & 0 & 1 & 0 & 0\\0 & 0 & 0 & 0 & 0 & 0 & 1 & 0\\0 & 0 & 0 & 0 & 0 & 0 & 0 & 1\\m_1 & 0 & 0 & 0 & 0 & 0 & 0 & 0\\-\mathrm{Gr} & s+M & 0 & 0 & 0 & 0 & -G & 0\\0 & 0 & m_2 & 0 & 0 & R & 0 & 0\\-m_3 & 0 & 0 & m_4 & 0 & 0 & 0 & 0\end{bmatrix}\begin{bmatrix}\bar{\theta}\\\bar{u}\\\bar{N}\\\bar{\Omega}\\\bar{\theta}'\\\bar{u}'\\\bar{N}'\\\bar{\Omega}'\end{bmatrix} \tag{18}$$

$$\frac{\mathrm{d}}{\mathrm{d}y}\bar{V}(y,s) = A(s)\bar{V}(y,s)$$

where

918

Ramya, E., *et al.*: Numerical and Analytical Comparisons of Slanted ...
THERMAL SCIENCE: Year 2019, Vol. 23, No. 2B, pp. 913-928

$$m_1 = \Pr s\left(1+\frac{4F}{3}\right)^{-1}, \quad m_2 = R_0 s + 2R, \quad m_3 = \frac{R_3}{R_2}\Pr s\left(1+\frac{4F}{3}\right)^{-1}, \quad \text{and} \quad m_4 = \frac{R_1}{2R_2}s+\frac{R_4}{R_2}$$

The formal solution of system of eq. (18) can be written in the structure:

$$\bar{V}(y,s) = \exp[A(s)y]\bar{V}(0,s) \tag{19}$$

The characteristic equation of the matrix A(s) has the form:

$$k^8 - (m_1+m_2+m_4-GR+s+M)k^6 + [M(m_1+m_2+m_4)+m_1 m_2 + m_1 m_4 + m_2 m_4 -$$
$$- GR(m_1+m_4)+s(m_1+m_2+m_4)]k^4 - [M(m_1 m_2 + m_1 m_4 + m_2 m_4)+m_1 m_2 m_4 +$$
$$+ GRm_1 + s(m_1 m_2 + m_1 m_4 + m_2 m_4)]k^2 + (s+M)(m_1 m_2 m_4) = 0 \tag{20}$$

The characteristic roots of eq. (20) are $\pm k_1, \pm k_2, \pm k_3, \pm k_4$ given by:

$$k_1^2 = m_1, \quad k_2^2 = m_4, \quad k_3^2 + k_4^2 = s + M + m_2 - GR, \quad k_3^2 k_4^2 = (s+M)m_2 \tag{21}$$

The Maclaurin series expansion of $\exp[A(s)y]$ is given by:

$$\exp[A(s)y] = \sum_{n=0}^{\infty} \frac{[A(s)y]^n}{n!}$$

Applying the Cayley-Hamilton theorem, we get:

$$A^8 - (m_1+m_2+m_4-GR+s+M)A^6 + [M(m_1+m_2+m_4)+m_1 m_2 + m_1 m_4 + m_2 m_4 -$$
$$- GR(m_1+m_4)+s(m_1+m_2+m_4)]A^4 - [M(m_1 m_2 + m_1 m_4 + m_2 m_4)+m_1 m_2 m_4 +$$
$$+ GRm_1 + s(m_1 m_2 + m_1 m_4 + m_2 m_4)]A^2 + (s+M)(m_1 m_2 m_4) = 0 \tag{22}$$

Equation (22) demonstrates that A^8 and all higher powers of A can be expressed in terms of A^7, A^6, A^5, A^4, A^3, A^2, A, and I, the unit matrix of order 8. The matrix exponential can be written in the structure:

$$\exp[A(s)y] = L(y,s) = a_0 I + a_1 A + a_2 A^2 + a_3 A^3 + a_4 A^4 + a_5 A^5 + a_6 A^6 + a_7 A^7 \tag{23}$$

Previous equation are presently evaluated by replacing the matrix A by its characteristic roots $\pm k_1, \pm k_2, \pm k_3$, and $\pm k_4$ leading to:

$$\exp(\pm k_1 y) = a_0 \pm a_1 k_1 + a_2 k_1^2 \pm a_3 k_1^3 + a_4 k_1^4 \pm a_5 k_1^5 + a_6 k_1^6 \pm a_7 k_1^7$$
$$\exp(\pm k_2 y) = a_0 \pm a_1 k_2 + a_2 k_2^2 \pm a_3 k_2^3 + a_4 k_2^4 \pm a_5 k_2^5 + a_6 k_2^6 \pm a_7 k_2^7$$
$$\exp(\pm k_3 y) = a_0 \pm a_1 k_3 + a_2 k_3^2 \pm a_3 k_3^3 + a_4 k_3^4 \pm a_5 k_3^5 + a_6 k_3^6 \pm a_7 k_3^7 \tag{24}$$
$$\exp(\pm k_4 y) = a_0 \pm a_1 k_4 + a_2 k_4^2 \pm a_3 k_4^3 + a_4 k_4^4 \pm a_5 k_4^5 + a_6 k_4^6 \pm a_7 k_4^7$$

By solving the system of linear eq. (24), we can determine $a_0 - a_7$. Substituting for the coefficients $a_0 - a_7$ into eqs. (23) and computing A^2, A^3, A^4, A^5, A^6 and A^7, one can acquire the entries $l_{ij}; i, j = 1,...8$ of the matrix $l(y,s)$ in the most straightforward conceivable

Ramya, E., *et al.*: Numerical and Analytical Comparisons of Slanted …
THERMAL SCIENCE: Year 2019, Vol. 23, No. 2B, pp. 913-928

919

structure. It is currently possible to solve a board class of problems in the Laplace transform domain.

The thermal shock problem

Consider the effects of thermal radiation MHD natural convection flow of a micro--stretch conducting liquid in a porous medium occupying a semi-infinite region $y > 0$ of the space bounded by an infinite vertical plate $y = 0$. Choosing the y-axis perpendicular to the surface of the plate, with the boundary conditions are:

$$\theta(0,t) = \theta_0 H(t), \quad \bar{\theta}(0,s) = \frac{\theta_0}{s}; \quad N(0,t) = 0, \qquad \bar{N}(0,s) = 0$$

$$u(0,t) = 0, \qquad \bar{u}(0,s) = 0; \quad \Omega(0,t) = 0, \qquad \Omega(0,s) = 0 \qquad (25)$$

where θ_0 is constant and $H(t)$ is Heaviside unit step function. Presently we apply the state--space approach previously described to this problem. Since the solution is bounded at infinity, the expressions for $l_{ij}; i, j = 1,...8$ can be gotten by smothering the positive exponential. This is equivalent to replacing each $\sinh(k_i y)$ by $-1/2\exp(-k_i y)$ and each $\cosh(k_i y)$ by $1/2\exp(-k_i y)$. In order to obtain the remaining four components $\theta'(0,s), \bar{u}'(0,s), \bar{N}'(0,s)$, and $\bar{\Omega}'(0,s)$, we substitute $y = 0$ into eqs. (19) to acquire the linear system of equations whose solution is given in the form:

$$\bar{\theta}'(0,s) = k_1 \frac{\theta_0}{s}, \quad \bar{u}'(0,s) = \frac{\mathrm{Gr}(k_3 + k_4)[k_3 k_4 + k_1(k_3 + k_4) + m_2] + \mathrm{Gr}\, k_1 GR}{(k_1 + k_3)(k_1 + k_4)[(k_3 + k_4)^2 + GR]},$$

$$\bar{\Omega}'(0,s) = -m_3 \frac{\theta_0}{s(k_1 + k_2)}, \quad \bar{N}'(0,s) = \frac{\mathrm{Gr}[k_3 k_4 + (s+M)]m_2 R}{k_3 k_4 (k_1 + k_3)(k_1 + k_4)[(k_3 + k_4)^2 + GR]} \qquad (26)$$

Finally, substituting the previous value into eq. (19), we acquire the solution of the problem in the transformed domain as:

$$\bar{\theta}(y,s) = \frac{\theta_0}{s} \exp(-k_1 y) \qquad (27)$$

$$\bar{u}(y,s) = \mathrm{A}_1 \exp(-k_4 y) + \mathrm{A}_2 \exp(-k_3 y) \qquad (28)$$

$$\bar{N}(y,s) = \mathrm{A}_3 \exp(-k_4 y) + \mathrm{A}_4 \exp(-k_3 y) \qquad (29)$$

$$\bar{\Omega}(y,s) = -\frac{\theta_0 m_3}{s(k_1 k_2 + k_2^2)} \exp(-k_2 y) \qquad (30)$$

where the constants $\mathrm{A}_i, i = 1,2,3,4,$ are listed in:

$$\mathrm{A}_1 = \frac{F_{11}}{k_4} \frac{\{k_4^2[(k_3^2 + k_4^2)(-k_2^2 + 3k_3^2 + k_4^2) - 2k_3^2(s+M)] + [-k_4^4 - 3k_3^2(s+M) - 4k_4^2(s+M) + 2(s+M)^2 + k_2^2(k_4^2 + (s+M))]\}M_2 + k_1^2 A_{1a}}{(k_1^2 - k_4^2)(k_4^2 - k_2^2)}$$

920

Ramya, E., *et al.*: Numerical and Analytical Comparisons of Slanted …
THERMAL SCIENCE: Year 2019, Vol. 23, No. 2B, pp. 913-928

$$A_2 = \frac{F_{11}}{k_3} \frac{\begin{array}{c} \{k_3^2[(k_3^2+k_4^2)(k_2^2-3k_4^2-k_3^2)+2k_4^2(s+M)]+[k_3^4+4k_3^2(s+M)+ \\ +3k_4^2(s+M)-2(s+M)^2-k_2^2[k_3^2+(s+M)]\}M_2+k_1^2 A_{2a} \end{array}}{(k_1^2-k_3^2)(k_3^2-k_2^2)}$$

$$A_3 = \frac{-F_{12}}{k_4} \frac{\begin{array}{c} \{k_1^2(k_2^2-k_4^2)(k_4^2-(s+M)]+k_4^2(-k_2^2+k_3^2+k_4^2)[k_3^2+k_4^2+(s+M)]+ \\ +(s+M)(k_2^2-k_3^2-2k_4^2+s+M)M_2 \end{array}}{(k_1^2-k_4^2)(k_2^2-k_4^2)}$$

$$A_4 = \frac{F_{12}}{k_3} \frac{\begin{array}{c} [k_1^2(k_2^2-k_3^2)(k_3^2-(s+M)]+k_3^2(-k_2^2+k_3^2+k_4^2)[k_3^2+k_4^2-(s+M)]+ \\ +(s+M)(k_2^2-k_3^2-2k_4^2+s+M)M_2 \end{array}}{(k_1^2-k_3^2)(k_2^2-k_3^2)}$$

$$A_{1a} = [-k_4^2(k_3^2+k_4^2)+k_2^2(k_4^2-m_2)+(k_4^2+s+M)m_2]$$

$$A_{2a} = [k_3^2(k_3^2+k_4^2)+k_2^2(-k_3^2+m_2)+(k_3^2+s+M)m_2]$$

$$F_{11} = \frac{\theta_0}{s} \frac{Gr\{(k_3+k_4)[k_3k_4+k_1(k_3+k_4)+m_2]+k_1 GR\}}{2(k_1+k_3)(k_3^2-k_4^2)(k_1+k_4)((k_3+k_4)^2+GR)}$$

$$F_{12} = -\frac{\theta_0}{s} \frac{Gr[k_3k_4+(s+M)]m_2 R}{2k_3k_4(k_1+k_3)(k_3^2-k_4^2)(k_1+k_4)[(k_3+k_4)^2+GR]}$$

The Shearing stress, τ_w, at the wall is given by:

$$\tau_w = \left|(\mu+\chi)\frac{\partial u}{\partial y}+\chi N\right|_{y=0} = -\rho\left|v\frac{\partial u}{\partial y}\right|_{y=0} \tag{31}$$

considering that $N(0,t)=0$. The skin-friction coefficient C_f is given:

$$C_f = \frac{\tau_w}{\frac{1}{2}\rho U^2} = -2\frac{\partial u}{\partial y} \tag{32}$$

Inversion of the Laplace transform

To invert the Laplace transform in previous equations, we may utilize a numerical procedure based on the Fourier expansion of a function [20]. In this method, the inverse $h(t)$ of the Laplace transform is approximated by the relation $\bar{h}(s)$:

$$h_N(t) = \frac{e^{dt}}{t_1}\left\{\frac{1}{2}\bar{h}(d)+Re\left[\sum_{k=1}^{\infty}e^{ik t\pi/t_1}\bar{h}\left(d+\frac{ik\pi}{t_1}\right)\right]\right\} \tag{33}$$

where d is a constant and N is a sufficiently large integer chosen such that:

Ramya, E., *et al.*: Numerical and Analytical Comparisons of Slanted ...
THERMAL SCIENCE: Year 2019, Vol. 23, No. 2B, pp. 913-928

921

$$\mathrm{e}^{\mathrm{d}t}\,\mathrm{Re}\left[\mathrm{e}^{iN t \pi / t_1}\overline{h}\left(d + \frac{iN\pi}{t_1}\right)\right] < \xi \tag{34}$$

where ξ is a preselected small positive number that corresponds to the degree of accuracy to be achieved. Equation (33) is the numerical inversion formula valid for $2t_1 \geq t \geq 0$. In particular, we choose $t = t_1$, to get:

$$h_N(t) = \frac{\mathrm{e}^{\mathrm{d}t}}{t_1}\left\{\frac{1}{2}\overline{h}(d) + \mathrm{Re}\left[\sum_{k=1}^{N}(-1)^k \overline{h}\left(d + \frac{ik\pi}{t_1}\right)\right]\right\} \tag{35}$$

Numerical procedure

The transient non-linear ordinary differential eqs. (9)-(12) subject to the initial and boundary conditions are solved numerically by Crank-Nicolson implicit finite different technique. The computational domain $(0 < t < \infty) - (0 < y < 1)$ is separated into a mesh of lines parallel to t- and y-axes. The finite difference approximation of (9)-(12) are acquired by substituting the approximations of derivatives. Thus, the governing equations and boundary conditions are changed into the following algebraic equations:

$$\frac{u_i^{j+1} - u_i^j}{\Delta t} = \frac{u_{i+1}^{j+1} - 2u_i^{j+1} + u_{i-1}^{j+1} + u_{i+1}^j - 2u_i^j + u_{i-1}^j}{2(\Delta y)^2} + G\frac{N_{i+1}^{j+1} - N_{i-1}^{j+1} + N_{i+1}^j - N_{i-1}^j}{4\Delta y} +$$
$$+ \frac{\mathrm{Gr}}{2}(\theta_i^{j+1} + \theta_i^j) - \frac{M}{2}(u_i^{j+1} + u_i^j) \tag{36}$$

$$R_0 \frac{N_i^{j+1} - N_i^j}{\Delta t} = \frac{N_{i+1}^{j+1} - 2N_i^{j+1} + N_{i-1}^{j+1} + N_{i+1}^j - 2N_i^j + N_{i-1}^j}{2(\Delta y)^2} -$$
$$- R\frac{u_{i+1}^{j+1} - u_{i-1}^{j+1} + u_{i+1}^j - u_{i-1}^j}{4\Delta y} - R(N_i^{j+1} + N_i^j) \tag{37}$$

$$\frac{R_1}{2}\frac{\Omega_i^{j+1} - \Omega_i^j}{\Delta t} = R_2\frac{\Omega_{i+1}^{j+1} - 2\Omega_i^{j+1} + \Omega_{i-1}^{j+1} + \Omega_{i+1}^j - 2\Omega_i^j + \Omega_{i-1}^j}{2(\Delta y)^2} +$$
$$+ R_3\frac{\theta_{i+1}^{j+1} - 2\theta_i^{j+1} + \theta_{i-1}^{j+1} + \theta_{i+1}^j - 2\theta_i^j - \theta_{i-1}^j}{2(\Delta y)^2} - R_4(\Omega_i^{j+1} + \Omega_i^j) \tag{38}$$

$$\mathrm{Pr}\frac{\theta_i^{j+1} - \theta_i^j}{\Delta t} = \frac{\theta_{i+1}^{j+1} - 2\theta_i^{j+1} + \theta_{i-1}^{j+1} + \theta_{i+1}^j - 2\theta_i^j + \theta_{i-1}^j}{2(\Delta y)^2} +$$
$$+ \frac{4F}{3}\frac{\theta_{i+1}^{j+1} - 2\theta_i^{j+1} + \theta_{i-1}^{j+1} + \theta_{i+1}^j - 2\theta_i^j + \theta_{i-1}^j}{2(\Delta y)^2} \tag{39}$$

and the associated initial and boundary conditions may be expressed:

$$u_i^1 = 0, \quad N_i^1 = 0, \quad \Omega_i^1 = 0, \quad \theta_i^1 = 0$$

$$u_1^j = 0, \quad N_1^j = 0, \quad \Omega_1^j = 0, \quad \theta_1^j = \theta_0 H(t) \tag{40}$$

where Δy and Δt are the mesh sizes along y and time directions, respectively. The computational domain $(0 < t < \infty)$ is divided into intervals with step size $\Delta t = 0.002$ for time (t). Here the subscript i designates the grid points with x-co-ordinate and j designates the value at a time $t = n\Delta t$, where $n = 1, 2, 3, \ldots$ *etc*. The accuracy and validation of the numerical procedure have been compared with the analytical results. It is seen from fig. 2 that the numerical results are in good agreement with analytical solutions.

Stability and convergence analysis

The stability criterion of the finite difference scheme for constant mesh sizes are examined using Von-Neumann technique as explained by Carnahan *et al.* [21]. The general terms of Fourier expansion for u, N, Ω, and θ are of the form:

$$u_i^j = \bar{u} G_a{}^j \mathrm{e}^{IKi}, \quad N_i^j = \bar{N} G_a{}^j \mathrm{e}^{IKi}, \quad \Omega_i^j = \bar{\Omega} G_a{}^j \mathrm{e}^{IKi}, \quad \theta_i^j = \bar{\theta} G_a{}^j \mathrm{e}^{IKi} \tag{41}$$

where $\bar{u}, \bar{N}, \bar{\Omega}, \bar{\theta}$ and K are constants and $I^2 = \sqrt{-1}$. The superscripts i, j are the grid points y and t, respectively. The finite difference eqs. (36)-(39) can be simplified by substituting eq. (41) and canceling the term $G_a{}^j \mathrm{e}^{IKi}$ in both sides. Thus the governing equations are:

$$G_a \bar{u} = \bar{u} \frac{E_2}{E_1} + \frac{G\Delta t I \sin k}{(1 + C_2)\Delta y E_1} \bar{N} + \frac{\mathrm{Gr}\,\Delta t\, C_4}{E_1} \bar{\theta}, \quad G_a \bar{\theta} = \bar{\theta} \frac{1 + C_4}{1 - C_4}$$

$$G_a \bar{N} = \bar{N} \frac{F_1}{1 - C_2} - \frac{E_1 + E_2}{E_1} F_2 \bar{u} - \frac{\mathrm{Gr}\,\Delta t\, C_4}{E_1} F_2 \bar{\theta}, \quad G_a \bar{\Omega} = \bar{\Omega} \frac{1 + C_3}{1 - C_3} + C_{3A} \bar{\theta} \tag{42}$$

where

$$C_1 = 1 + \frac{\Delta t(\cos k - 1)}{(\Delta y)^2} - \frac{M\Delta t}{2}, \quad E_1 = (1 - C_1) + \frac{G\Delta t I \sin k}{2\Delta y} \frac{RI \sin k \Delta t}{2R_0 \Delta y (1 - C_2)}$$

$$C_2 = \frac{\Delta t(\cos k - 1)}{R_0 (\Delta y)^2} - \frac{2R\Delta t}{R_0} - \frac{RI \sin k \Delta t}{2R_0 \Delta y} \frac{G\Delta t I \sin k}{2(1 - C_1)\Delta y}$$

$$E_2 = (1 + C_1) + \frac{G\Delta t I \sin k}{2\Delta y} \frac{RI \sin k \Delta t}{2R_0 \Delta y (1 - C_2)}, \quad C_3 = \frac{2R_2 \Delta t}{R_1} \frac{\cos k - 1}{(\Delta y)^2} + \frac{2R_4 \Delta t}{R_1}$$

$$C_{3A} = \frac{4R_3 \Delta t}{R_1 (1 - C_4)(1 - C_3)} \frac{\cos k - 1}{(\Delta y)^2}, \quad F_1 = (1 + C_2) - \frac{R\Delta t I \sin k}{2R_0 \Delta y} \frac{G\Delta t I \sin k}{E_1 \Delta y (1 + C_2)}$$

$$C_4 = \frac{\Delta t}{\mathrm{Pr}} \left(1 + \frac{4F}{3}\right) \frac{\cos k - 1}{(\Delta y)^2}, \quad F_2 = \frac{RI \Delta t \sin k}{2R_0 \Delta y (1 - C_2)}$$

The system of eq. (42) can be written in matrix form:

$$\begin{bmatrix} G_a \bar{u} \\ G_a \bar{N} \\ G_a \bar{\Omega} \\ G_a \bar{\theta} \end{bmatrix} = \begin{bmatrix} a_{11} & a_{12} & a_{13} & a_{14} \\ a_{21} & a_{22} & a_{23} & a_{24} \\ a_{31} & a_{32} & a_{33} & a_{34} \\ a_{41} & a_{42} & a_{43} & a_{44} \end{bmatrix} \begin{bmatrix} \bar{u} \\ \bar{N} \\ \bar{\Omega} \\ \bar{\theta} \end{bmatrix} \tag{43}$$

Ramya, E., *et al.*: Numerical and Analytical Comparisons of Slanted ...
THERMAL SCIENCE: Year 2019, Vol. 23, No. 2B, pp. 913-928

923

where

$$a_{11} = \frac{E_2}{E_1}, \quad a_{12} = \frac{G\,\Delta t\, I \sin k}{(1+C_2)\Delta y E_1}, \quad a_{14} = \frac{\mathrm{Gr}\,\Delta t\, C_4}{E_1}, \quad a_{21} = -F_2 \frac{E_1+E_2}{E_1},$$

$$a_{22} = \frac{F_1}{(1-C_2)}, \quad a_{24} = -F_2 \frac{-\mathrm{Gr}\,\Delta t\, C_4}{E_1}, \quad a_{33} = \frac{1+C_3}{1-C_3}, \quad a_{34} = C_{3A}, \quad a_{44} = \frac{1+C_4}{1-C_4}$$

The Eigen values of the previous matrix are:

$$\lambda_1 = \frac{1+C_4}{1-C_4}, \quad \lambda_3 = \frac{1}{2}\left[\frac{E_2}{E_1} + \frac{F_1}{1-C_2} - \sqrt{\left(\frac{E_2}{E_1} - \frac{F_1}{1-C_2}\right)^2 - 4F_2 \frac{E_1+E_2}{E_1} \frac{G\Delta t I \sin k}{E_1(1+C_2)\Delta y}}\right],$$

$$\lambda_2 = \frac{1+C_3}{1-C_3}, \quad \lambda_4 = \frac{1}{2}\left[\frac{E_2}{E_1} + \frac{F_1}{1-C_2} + \sqrt{\left(\frac{E_2}{E_1} - \frac{F_1}{1-C_2}\right)^2 - 4F_2 \frac{E_1+E_2}{E_1} \frac{G\Delta t I \sin k}{E_1(1+C_2)\Delta y}}\right] \quad (44)$$

The constant C_1 can be represented:

$$C_1 = 1 + 2\frac{\Delta t\left(\sin^2 \frac{k}{2}\right)}{(\Delta y)^2} - \frac{M\,\Delta t}{2}$$

and the real part of C_1 is greater than or equal to zero. Similarly, the real part of C_2, C_3, and C_4 are greater than or equal to zero. Therefore, $|\lambda_n| \leq 1, n = 1, 2, 3, 4$, and the scheme is unconditionally stable. The local truncation error $O(\Delta t^2 + \Delta y^2)$ is and it tends to zero as Δt and Δy tend to zero. Hence, the scheme is compatible. Stability and compatibility ensures convergence.

Results and discussion

Slanted hydromagnetic boundary-layer flow with heat transfer and natural convection flow of a micropolar fluid with stretch past a porous plate subjected to prescribed heat flux embedded in a porous medium in the presence of thermal radiation and a slanted magnetic field is examined in this work. Governing boundary-layer equations are solved analytically by using the state-space approach. The technique is applied to the 1-D thermal shock problem for the half-space. The solutions are obtained for different values of physical parameters which arise in the study and are illustrated graphically in figs. 2 to 11 to analyze their effects over the velocity, microrotation, micro-stretch, and temperature. The computational work of the problem is carried out using MATLAB and the computations were performed for the constants of the problem namely

$$M_1 = 2, \quad \omega = 45°, \quad F = 1, \quad K = 1.5, \quad R = 8, \quad G = 2, \quad R_0 = 1.3, \quad R_1 = 1.3,$$

$$R_2 = 0.001, \quad R_3 = 0.5, \quad R_4 = 0.5, \quad t = 3, \quad \mathrm{Gr} = 2$$

We have obtained a comprehensive range of solutions to the transformed conservation equations. In order to check the accuracy of the present results, the present analytical solution has been validated the numerical results of Crank Nicolson method, which is shown in fig. 2. It is clearly seen from figure that the results are in good agreement. As the precision of the numerical solutions is great, the analytical and numerical solutions are very close to each

924

Ramya, E., *et al.*: Numerical and Analytical Comparisons of Slanted …
THERMAL SCIENCE: Year 2019, Vol. 23, No. 2B, pp. 913-928

other in the velocity profile. Figure 2 demonstrates that the stream velocity is found to accelerate with natural convection parameter Gr from 2.0 to 6.0.

The simultaneously effects of magnetic parameter and aligned angle on the velocity profile are appeared in fig. 3. It is noticed that an augmentation in the aligned angle of magnetic field and the magnetic parameter decelerates the velocity profile. Here $\omega = 0°$ symbolizes to the case where there is no impact of magnetic field in the stream area and $\omega = 90°$ symbolizes to the case where the magnetic field acts transversely on the stream area. The rising values of aligned angle ($0°$-$90°$) lead to enhance the magnetic field strength in the stream area. Because of upgrade of magnetic field strength, a resistive type force called Lorentz force connected with the aligned magnetic field makes the boundary-layer more slender furthermore the magnetic field lines of force move past the porous plat at the free stream velocity. The thickness of velocity boundary-layer gets to be more slender as the magnetic field strength expands which is clear because of stream gets stifled by the magnetic field.
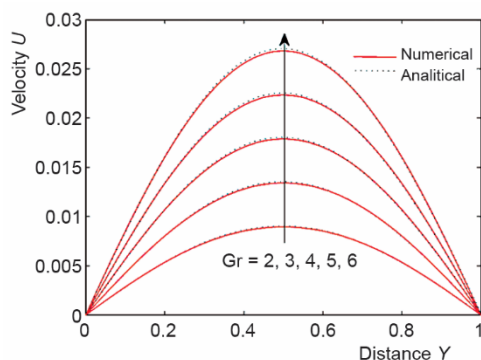
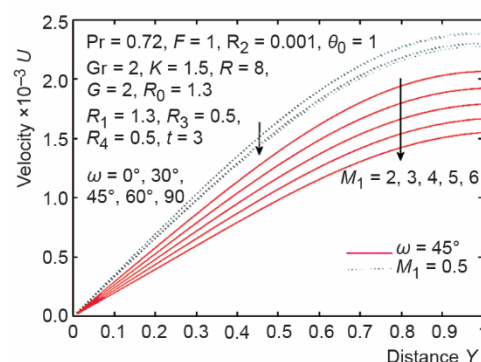**Figure 2. Comparative study of velocity profiles for different Gr**

Figure 3. Velocity distribution for different values of M_1 and ω

The flow of liquids over the boundaries has numerous applications, for example, boundary-layers control. The investigation of transient boundary-layers owes its significance to the fact that all boundary-layers that occur in real life are, in a sense, unsteady. Lately, the requirements of modern technology have stimulated interest in liquid-flow studies, which involve the intersection of few phenomena. One such study is related to the impacts of natural convection flow through a porous medium, which play a vital part in agriculture, engineering, petroleum industries, and heat transfer.

Figure 4 demonstrates the impact of the permeability of the porous medium K on the velocity dispersion. As appeared, the velocity increases with an increase in dimensionless porous medium parameter. This is because of the way that increasing values of K diminishes the drag force which helps the liquid extensively to move quickly. Figure 5 illustrates that the velocity profile for different values of the thermal radiation parameter F in the boundary-layer. Clearly, an increase in the thermal radiation F results an enhancement in the external velocity, thermal radiation is dispersed more quickly to the surrounding hence increasing the velocity boundary layer and also the thickness of momentum boundary-layers.

The influence of the magnetic parameter M_1 and aligned angle ω on the microrotation profile with fixed values of other parameters is depicted in fig. 6. It can be seen that the effect of increasing the values of magnetic parameter and aligned angle are to decrease the

Ramya, E., *et al.*: Numerical and Analytical Comparisons of Slanted …
THERMAL SCIENCE: Year 2019, Vol. 23, No. 2B, pp. 913-928

925

microrotation profile near the plate $(0 \leq Y \leq 1)$. This is due to the fact that the transverse magnetic field gives rise to a resistive-type of force, called Lorentz force. This force has the tendency to slow down the motion of the fluid which results in reducing the micro-rotation profiles.
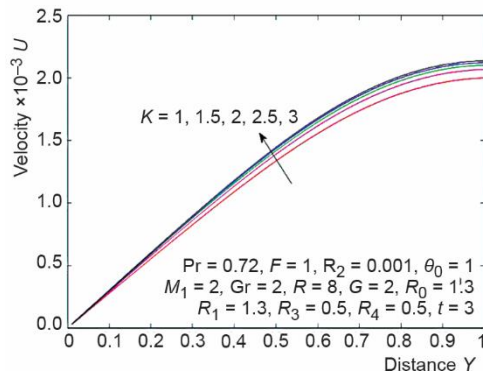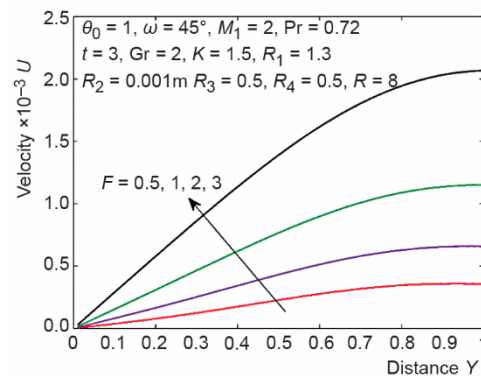

Figure 4. Velocity distribution for different values of *K*

Figure 5. Velocity distribution for different values of *F*
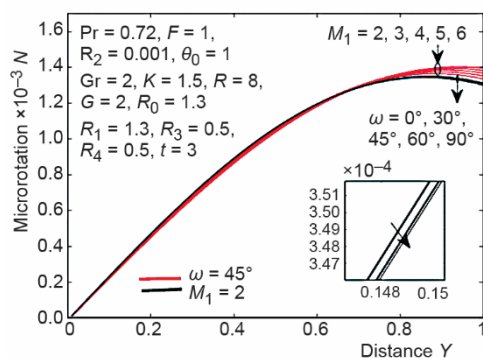
Figure 6. Microrotation distribution for different values of M_1 and ω
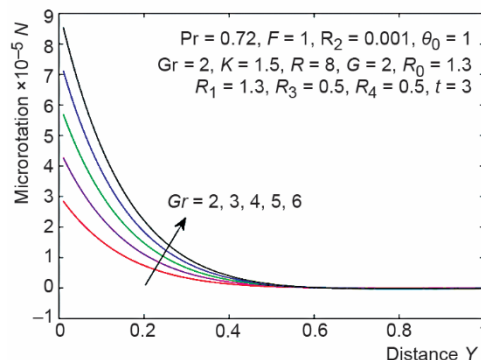
Figure 7. Microrotation distribution for different values of Gr

The micro-rotation profile for various values of Grashof number are portrayed in fig. 7. It is observed that an increase in Grashof number leads to increase in the values of microrotation. Here Grashof number represents that the effects of natural convection currents. Physically, $Gr > 0$ represent that the cooling fluid is heated in the boundary surface, whereas $Gr < 0$ means that the hot fluid is cooled in the boundary surface. In addition $Gr = 0$ denotes to the absence of natural convection currents. Also, the curves demonstrates that the peak value of velocity increases quickly close to the wall of the porous plate as Grashof number increases, and afterward decomposes to the free stream micro-rotation. Figure 8 portrays the effect of the Prandtl number on the micro-stretch profiles of the stream field for two values of time, to be specific, $t = 3$ and $t = 7$, and keeping different parameters of the stream field constant. The Prandtl number is found to improve the micro-stretch of the stream field at all points while the time is found to decelerate the micro-stretch field. The effect of coupled pa-

rameter R_4 over the dimensionless micro-stretch is demonstrated in fig. 9. Increase in coupled parameter R_4 is accompanied with decrease in micro-stretch distribution and micro-stretch boundary-layer thickness become thinner.
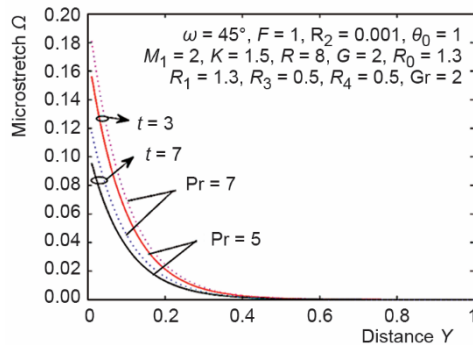

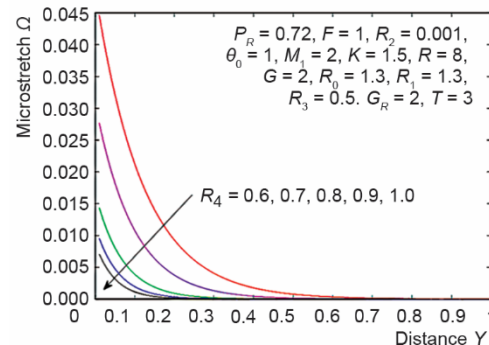**Figure 8. Micro-stretch distribution for different values of Pr and t**

Figure 9. Micro-stretch distribution for different values of R_4

The temperature profile for some reasonable values of Pr = 0.72, 2.0, 5.0, 7.0, which are essential as in the physically compare to air, gas, R-12 refrigerant and water are exposed in fig. 10. In fig. 10, we observe that the temperature reduces with mounting values of Prandtl number. It is likewise observed that the thermal boundary-layer thickness is most extreme close to the plate and decreases with increasing distances from the leading edge lastly ways to deal with zero. Besides, it is seen that the thermal boundary-layer for air which related to Pr = 0.72 is more prominent than those for air, gas, R-12 refrigerant, and water. It is defended because of the way that thermal conductivity of fluid declines with increasing Prandtl number and henceforth diminishes the thermal boundary-layer thickness and the temperature profiles. The temperature profile for different values of thermal radiation parameter F is plotted in fig. 11. This figure demonstrates that the effect of thermal radiation is to improve heat transfer due to the way that thermal boundary-layer thickness increments with enhance in the thermal radiation. Above these lines, it is noted that, the radiation must be reduced to get the cooling process at a maximum rate.
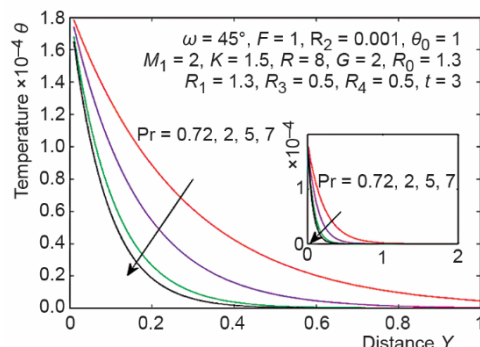

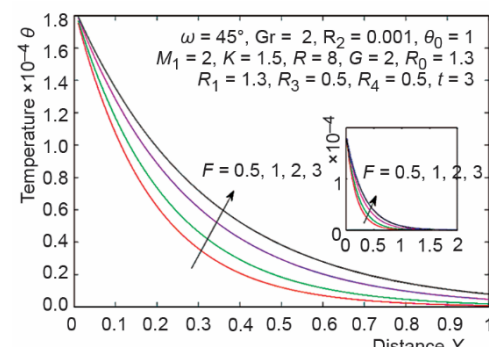**Figure 10. Temperature distribution for different values of Pr**

Figure 11. Temperature distribution for different values of F

Conclusions

The influence of thermal radiation on slanted MHD heat transfer flow of a micro--stretch fluid past an infinite vertical porous plate is studied systematically and numerically. In this work, the idea of state-space methodology is briefly acquainted and employed to derive solutions of non-linear equations [22]. The acquired results from state-space approach are compared with from numerical method (Crank-Nicolson implicit finite different technique) to confirm the uniqueness of the proposed method. The outcomes uncover that the state-space approach can accomplish appropriate results in anticipating the solutions of such problems.

The velocity of momentum boundary-layer thickness declines with the increasing values of aligned angle of magnetic field, ω, and magnetic parameter, M_1. The microrotation profile also diminishes with increasing values of aforementioned parameters. The aligned angle of the magnetic field plays an essential part in controlling the magnetic field strength and the effect of Lorentz force on the micro-stretch fluid flow region. The effect of Grashof number is to enhance the non-dimensional velocity and temperature for its increasing values individually.

The effect of permeability parameter, K, is to increase the velocity as well as to increase the momentum boundary-layer thickness. Variable permeability has more tendencies to control the fluid velocity than uniform permeability. An increase in the thermal radiation parameter, F, is to increase the thickness of the velocity, temperature as well as thermal boundary-layer thickness. The micro-stretch profile decreases with an increase in the values of coupled parameter R_4. An increase in the Prandtl number is to increase the micro-stretch for both lower and higher values of time parameter t.

Acknowledgment

Nomenclature

B_0 – magnetic induction, [kg^{2}m^{-2}s^{-1}]
C_f – skin-friction coefficient
j – micro-inertia density
L – enclosure length, [m]
T_w – temperature of the heated surface, [K]
T_∞ – temperature of the ambient fluid, [K]
t – time
u, v – velocity components in the x- and y-directions, [ms^{-1}]
U – characteristic velocity, [ms^{-1}]

Greek symbols

γ – spin-gradient viscosity
θ – dimensionless temperature
μ – fluid viscosity, [kgm^{-1}s^{-1}]
μ_e – magnetic permeability of the fluid
ρ – density of the fluid, [kgm^{-3}]
σ – electric conductivity, [kgs^{-2}]
χ – vortex viscosity

References

[1] Eringen, A. C., Theory of Micropolar Fluids with Stretch, *Int. J. Eng. Sci., 7* (1969), 1, pp. 115-125
[2] Eringen, A. C., Simple of Micro-Fluids, *Int. J. Eng. Sci., 2* (1964), 2, pp. 205-217
[3] Eringen, A. C., Theory of Microstretch Liquid Crystals, *J. Math. Phys., 23* (1992), 12, pp. 4078-4086
[4] Sherief, H. H., *et al.*, Galerkin Representations and Fundamental Solutions for an Axisymmetric Microstretch Fluid Flow, *J. Fluid Mech., 619* (2009), Jan., pp. 277-293

928

Ramya, E., *et al.*: Numerical and Analytical Comparisons of Slanted …
THERMAL SCIENCE: Year 2019, Vol. 23, No. 2B, pp. 913-928

[5]   Narasimhan, M. N., A Mathematical Model of Pulsatile Flows of Microstretch Fluid in circular Tubes, *Int. J. Eng. Sci., 41* (2003), 3-5, pp. 231-247
[6]   Ezzat, M. A., El-Sapa, S., State space Approach to Magnetohydrodynamic Flow of Perfectly Conducting Micropolar Fluid with Stretch, *Int. J. Numer. Meth. Fluids, 70* (2012), 1, pp. 114- 134
[7]   Abdul Hakeem, A. K., *et al.*, Influence of Inclined Lorentz Forces on Boundary Layer Flow of Casson Fluid over an Impermeable Stretching Sheet with Heat Transfer, *J. Magn. Magn. Mater., 401* (2016), Mar., pp. 354-361
[8]   Punnamchandar, B., Iyengar, T. K. V., Pulsating Flow of an Incompressible Micropolar Fluid between Permeable Beds with an Inclined Uniform Magnetic Field. *Eur. J. Mech. B Fluids, 48* (2014), Nov., pp. 174-182
[9]   Yanhai, L., *et al.*, Magnetohydrodynamic thin Film and Heat Transfer of Power Law Fluids over an Unsteady Stretching Sheet with Variable Thermal Conductivity, *Thermal Science, 20* (2016), 6, pp. 1791-1800
[10] Helmy, K. A., *et al.*, MHD Free Convection Flow of a Micropolar Fluid Past a Vertical Porous Plate, *Can. J. Phys., 80 (*2002), 12, pp. 1661-1673
[11] Pal, D., Chatterjee, S., Heat and Mass Transfer in MHD Non-Darcian Flow of a Micropolar Fluid over Astretching Sheet Embedded in a Porous Media with Non-Uniform Heat Source and Thermal Radiation, *Commun. Nonlinear Sci. Numer. Simul., 15* (2010), 7, pp. 1843-1857
[12] Ibrahim, F. S., *et al.*, Effect of the Chemical Reaction and Radiation Absorption on the Unsteady MHD Free Convection Flow Past a Semi Infinite Vertical Permeable Moving Plate with Heat Source and Suction, *Commun. Nonlinear Sci. Numer. Simul., 13* (2008), 6, pp. 1056-1066
[13] Shit, G. C., *et al.*, Unsteady Flow and Heat Transfer of a MHD Micropolar Fluid over a Porous Stretching Sheet in the Presence of Thermal Radiation, *J. Mech., 29* (2013), 3, pp. 559-568
[14] Abo-Eldahab, E. M., Ghonaim, A. F., Radiation Effect on Heat Transfer of a Micropolar Fluid Through a Porous Medium, *Appl. Math. Comput., 169* (2005), 1, pp. 500-510
[15] Rahman, A. M., Sultan, T., Radiative Heat Transfer Flow of Micropolar Fluid with Variable Heat Flux in a Porous Medium, *Nonlinear Anal: Model. Control, 13* (2008), 1, pp. 71-87
[16] Das, K., Effect of Chemical Reaction and Thermal Radiation on Heat and Mass Transfer Flow of MHD Micropolar Fluid in a Rotating Frame of Reference, *Int. J. Heat Mass Transf., 54* (2011), 15, pp. 3505-3513
[17] Muthtamilselvan, M., *et al.*, Effect of Radiation on Transient MHD Flow of Micropolar Fluid between Porous Vertical Channel with Boundary Conditions of the Third Kind, *Ain Shams Eng. J., 5* (2014), 4, pp. 1277-1286
[18] Muthtamilselvan, M., *et al.*, Transient Heat And Mass Transfer Of Micropolar Fluid Between Porous Vertical Channel With Boundary Conditions Of Third Kind, *Int. J. Nonlinear Sci. Numer. Simul., 17* (2016), 5, pp. 231-242
[19] Ezzat, M. A., *et al.*, A Problem of a Micropolar Magnetohydrodynamic Boundary Layer Flow, *Can. J. Phys., 77* (2000), 10, pp. 813-827
[20] Honig, G., Hirdes, U., A Method for the Numerical Inversion of Laplace Transforms, *J. Comput. Appl. Math., 10* (1984), 1, pp. 113-132
[21] Carnahan, B., *et al.*, *Applied Numerical Methods*, John Wily and Sons, New York, USA, 1969
[22] Ezzat, M. A., *et al.*, State Space Formulation to Viscoelastic Fluid Flow of Magnetohydrodynamic Free Convection through a Porous Medium, *Acta Mech., 119* (1996), 1, pp. 147-164